PNAS RESEARCH ARTICLE | CELL BIOLOGY

S-lactoyl modification of KEAP1 by a reactive glycolytic metabolite activates NRF2 signaling

Yeonjin Ko[a,1], Mannkyu Hong[a,1], Seungbeom Lee[a,1], Manoj Kumar[b], Lara Ibrahim[a,c], Kayla Nutsch[a], Caroline Stanton[a,c], Phillip Sondermann[a], Braddock Sandoval[a], Maya L. Bulos[a], Jonathan Iaconelli[a], Arnab K. Chatterjee[b], R. Luke Wiseman[c], Peter G. Schultz[a,b,2], and Michael J. Bollong[a,2]

Contributed by Peter G. Schultz; received January 13, 2023; accepted April 5, 2023; reviewed by Nathanael S. Gray and Kevan M. Shokat

KEAP1 (Kelch-like ECH-associated protein), a cytoplasmic repressor of the oxidative stress responsive transcription factor Nuclear factor erythroid 2-related factor 2 (NRF2), senses the presence of electrophilic agents by modification of its sensor cysteine residues. In addition to xenobiotics, several reactive metabolites have been shown to covalently modify key cysteines on KEAP1, although the full repertoire of these molecules and their respective modifications remain undefined. Here, we report the discovery of sAKZ692, a small molecule identified by high-throughput screening that stimulates NRF2 transcriptional activity in cells by inhibiting the glycolytic enzyme pyruvate kinase. sAKZ692 treatment promotes the buildup of glyceraldehyde 3-phosphate, a metabolite which leads to S-lactate modification of cysteine sensor residues of KEAP1, resulting in NRF2-dependent transcription. This work identifies a posttranslational modification of cysteine derived from a reactive central carbon metabolite and helps further define the complex relationship between metabolism and the oxidative stress-sensing machinery of the cell.

intrinsically reactive metabolite | posttranslational modification | glycolysis | pyruvate kinase

Nuclear factor erythroid 2-related factor 2, NRF2, is a cap'n'collar (CNC) basic leucine zipper transcription factor (TF) that serves as the master regulator of oxidative stress resistance in mammalian cells (1, 2). Among CNC TFs, NRF2 is unique in that under normal circumstances it is continually sent for proteasomal degradation in the cytoplasm via its interactions with its repressor protein and cullin 3 E3 ligase adaptor KEAP1 (Kelch-like ECH-associated protein) (3). In the presence of oxidative stress or electrophilic agents, however, covalent modification of several cysteine "sensor" residues in KEAP1 by oxidation or by alkylation results in decreased ubiquitination and degradation of NRF2 (4, 5). NRF2 buildup serves as a licensing signal for its phosphorylation and translocation to the nucleus where it promotes the upregulation of transcripts containing antioxidant response elements (AREs) in their genetic regulatory sequences (6). Core NRF2 target transcripts include those related to glutathione (GSH) synthesis and recycling, reactive oxygen species elimination, and NADPH generation, among others (3). The net result of NRF2 activation is cellular resilience in the presence of oxidative and inflammatory insult. As such, mechanisms for regulating the activity of NRF2 are of key physiological and therapeutic importance.

In addition to electrophilic xenobiotic chemicals, several endogenous, intrinsically reactive metabolites have also been found to form covalent adducts with KEAP1 sensor residues and thereby activate NRF2. In 2011, two groups linked the common occurrence of fumarate hydratase mutations in hereditary leiomyomatosis and renal cell carcinoma (HLRCC) to the buildup of the citric acid (TCA) cycle metabolite fumarate (7, 8). Fumarate buildup in HLRCC promotes the covalent succinylation of KEAP1 C151 and C288, serving to activate NRF2 in renal cysts and promote tumor cell survival. Another TCA-derived metabolite, itaconate, has been shown to be produced by lipopolysaccharide (LPS)-stimulated macrophages, also resulting in the alkylation of KEAP1 C151 (9). Activation of NRF2 by itaconate has been shown to decrease innate immune signaling, providing a negative regulatory feedback stimulus in response to macrophage activation.

More recently, we described the identification of CBR-470-1, a nonelectrophilic small-molecule activator of NRF2 transcriptional activity (10, 11). This compound inhibits the glycolytic enzyme phosphoglycerate kinase (PGK1) in cells, leading to the buildup of triose phosphates and their degradation product methylglyoxal (MGx). MGx nonenzymatically cross-links proximal KEAP1 molecules via a methyl imidazole-based linkage between cysteine (C151) and arginine (R15 or R135) residues, a posttranslational modification we termed MICA (methylimidazole crosslink of cysteine and arginine) (10). This work uncovered the existence of direct interpathway communication between glycolysis and the KEAP1–NRF2 axis, suggesting the likelihood that NRF2 activation in this context serves to diminish the levels of potentially harmful glycolytic metabolites.

Significance

Several reactive endogenous metabolites have been shown to activate the NRF2-driven oxidative stress response in mammalian cells. Here, we expand this repertoire of reactive metabolites by showing that pharmacological inhibition of pyruvate kinase, the last step in glycolysis, results in the accumulation of glyceraldehyde 3-phosphate, a metabolite that results in the covalent modification and inactivation of the NRF2 repressor protein KEAP1. This work identifies a nonenzymatically derived posttranslational modification of cysteine, termed S-lactoylation, and further builds upon existing data that glycolysis directly communicates to the KEAP1–NRF2 signaling pathway through reactive metabolite-derived modifications of cysteine.

Author affiliations: [a]Department of Chemistry, The Scripps Research Institute, San Diego, CA 92037; [b]Calibr, A Division of Scripps Research, San Diego, CA 92037; and [c]Department of Molecular Medicine, The Scripps Research Institute, San Diego, CA 92037

Author contributions: Y.K., M.H., S.L., M.K., A.K.C., R.L.W., P.G.S., and M.J.B. designed research; Y.K., M.H., S.L., M.K., L.I., K.N., C.S., J.I., and M.J.B. performed research; Y.K., M.H., P.S., B.S., M.L.B., P.G.S., and M.J.B. analyzed data; and M.H., P.G.S., and M.J.B. wrote the paper.

Reviewers: N.S.G., Stanford Medicine; and K.M.S., University of California San Francisco.

The authors declare no competing interest.

Copyright © 2023 the Author(s). Published by PNAS. This article is distributed under Creative Commons Attribution-NonCommercial-NoDerivatives License 4.0 (CC BY-NC-ND).

[1]Y.K., M.H., and S.L. contributed equally to this work.

[2]To whom correspondence may be addressed. Email: schultz@scripps.edu or mbollong@scripps.edu.

This article contains supporting information online at https://www.pnas.org/lookup/suppl/doi:10.1073/pnas.2300763120/-/DCSupplemental.

Published May 8, 2023.

We hypothesized that other mechanisms for activating NRF2 by reactive metabolites likely exist, given the number of putative thiol-reactive metabolites that are present at high levels in mammalian cells. To further interrogate the cell for such mechanisms, here we performed an expanded high-throughput chemical screen for non-electrophilic small-molecule activators of NRF2 activity, reasoning that some fraction of hit molecules may act by promoting the buildup of KEAP1-reactive metabolites. From this effort, we identified a pharmacological inhibitor of glycolysis, which, instead of promoting MGx-based modification of KEAP1-like CBR-470-1, resulted in the buildup of an alternative glycolytic metabolite that promotes a non-enzymatically derived posttranslational modification of cysteines in KEAP1.

Results

Discovery of sAKZ692, a Nonreactive Small-Molecule NRF2 Activator. To identify additional pharmacological mechanisms for stimulating NRF2, we used a 1536-well compatible luciferase-based reporter assay for measuring ARE activation in IMR32 cells (ARE-LUC). From a screen of nearly 600,000 compounds, we identified 760 compounds that dose dependently increased ARE-LUC activity (*SI Appendix*, Fig. S1 *A–C*). Of these, 71 compounds did not bear any known cysteine-reactive chemical moieties (*SI Appendix*, Fig. S1*D*), and among the most efficacious of these putative noncovalent activators were eight indole-containing molecules elected for further study (*SI Appendix*, Fig. S1*E*). From a structure–activity relationship study of related commercially available molecules, a tryptamine-based pharmacophore was found to activate ARE-LUC most potently among compounds of this class (*SI Appendix*, Fig. S1*E*). Considerable tolerability for substitution of the "Eastern" moieties (as depicted in *SI Appendix*, Fig. S1 *E* and *F*) was additionally demonstrated. sAKZ692 (Fig. 1*A*) was found to be the most efficacious of these molecules, displaying low micromolar potency (2.2 μM) in ARE-LUC assays in IMR32 cells with no significant cytotoxicity (>20 μM, CellTiterGlo-based) over 24 h of treatment (Fig. 1*B*). Unlike the covalent NRF2 activator dimethyl fumarate (also called BG-12), sAKZ692 did not form adducts with GSH in vitro when measured by liquid chromatography–mass spectrometry (LC–MS, *SI Appendix*, Fig. S1*G*). sAKZ692 treatment also dose and time dependently increased levels of the NRF2-controlled transcripts *NQO1* and *HMOX1* in IMR32 cells (*SI Appendix*, Fig. S1*G*). Additionally, when IMR32 cells were evaluated for transcriptome-wide changes by RNA sequencing, sAKZ692 treatment (20 μM) was found to induce a selective and robust NRF2 transcriptional profile as assessed by gene set enrichment analysis (GSEA) using commonly used NRF2 gene sets (Fig. 1 *C–F*). Together, these data indicated that sAZK692 activates NRF2 in cells, most likely via a mechanism other than direct covalent modification of KEAP1.

sAKZ692 Is an Inhibitor of Pyruvate Kinase. To identify the cellular target of sAKZ692, we generated a photoactivatable affinity probe, sCLA626, which retained ARE-LUC-inducing activity in IMR32 cells (EC_{50} = 3.3 μM; Fig. 2 *A* and *B*). Treatment of IMR32 cells with sCLA626 followed by ultraviolet (UV) cross-linking and click-reaction-based conjugation with rhodamine azide revealed a predominantly labeled band near 58 kDa (*SI Appendix*, Fig. S2*A*). Liquid chromatography–tandem mass spectrometry-based analysis of excised gel slices indicated that this band corresponded to the enzyme pyruvate kinase. Pyruvate kinase catalyzes the last step in glycolysis, irreversibly promoting phosphoryl transfer from phosphoenolpyruvate to adenosine diphosphate (ADP) to yield pyruvate and adenosine triphosphate (ATP) (12). The broadly expressed pyruvate kinase gene encodes two isoforms, M1 and M2 (called PKM1 and PKM2), which differ by the inclusion of exon 12 in the carboxy terminus of the M2 isoform. Inclusion of exon 12 enables allosteric activation of PKM2 by fructose-1,6 bisphosphate (FBP) as well as the ability of PKM2 to form homotetramers, which display higher specific activity than the monomeric or dimeric forms (12). Using recombinant preparations of these enzymes, we found that sCLA626 dose dependently labeled both PKM1 and PKM2 with similar efficiencies in vitro (Fig. 2*C*), indicating that sAKZ692 can likely engage both isoforms of the protein. RNA-sequencing data from IMR32 cells showed that splice junction reads pertaining to PKM2 were markedly increased (>20-fold; *SI Appendix*, Fig. S2*B*) relative to those pertaining to PKM1, suggesting that most of the pyruvate kinase in IMR32 cells was the PKM2 isoform. This result is consistent with literature suggesting that PKM2 is the predominant isoform in proliferating cells (13). Accordingly, we focused our efforts on PKM2.

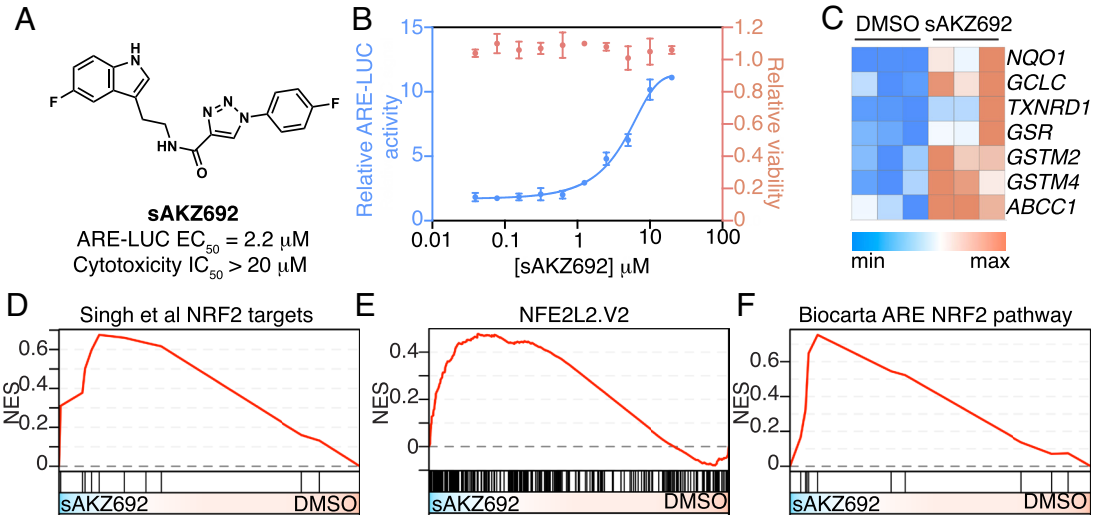

Fig. 1. sAKZ692, a pharmacological activator of NRF2-driven transcription. (*A*) Structure and activity of sAKZ692. (*B*) Relative ARE-LUC activity and cellular viability in response to 24-h treatment of IMR32 cells with the indicated concentrations of sAKZ692 (n = 3; mean and SEM). (*C*) Heatmap of up-regulated NRF2 controlled transcripts as assessed by RNA-seq after 24-h treatment of IMR32 cells with sAKZ692 (n = 3; 20 μM). (*D–F*) GSEA plots of NRF2-dependent gene sets (MSigDB IDs: M2662, M2870, M14339) from IMR32 cells treated for 24 h with sAKZ692 [20 μM; P < 0.0001, (nominal value), GSEA].

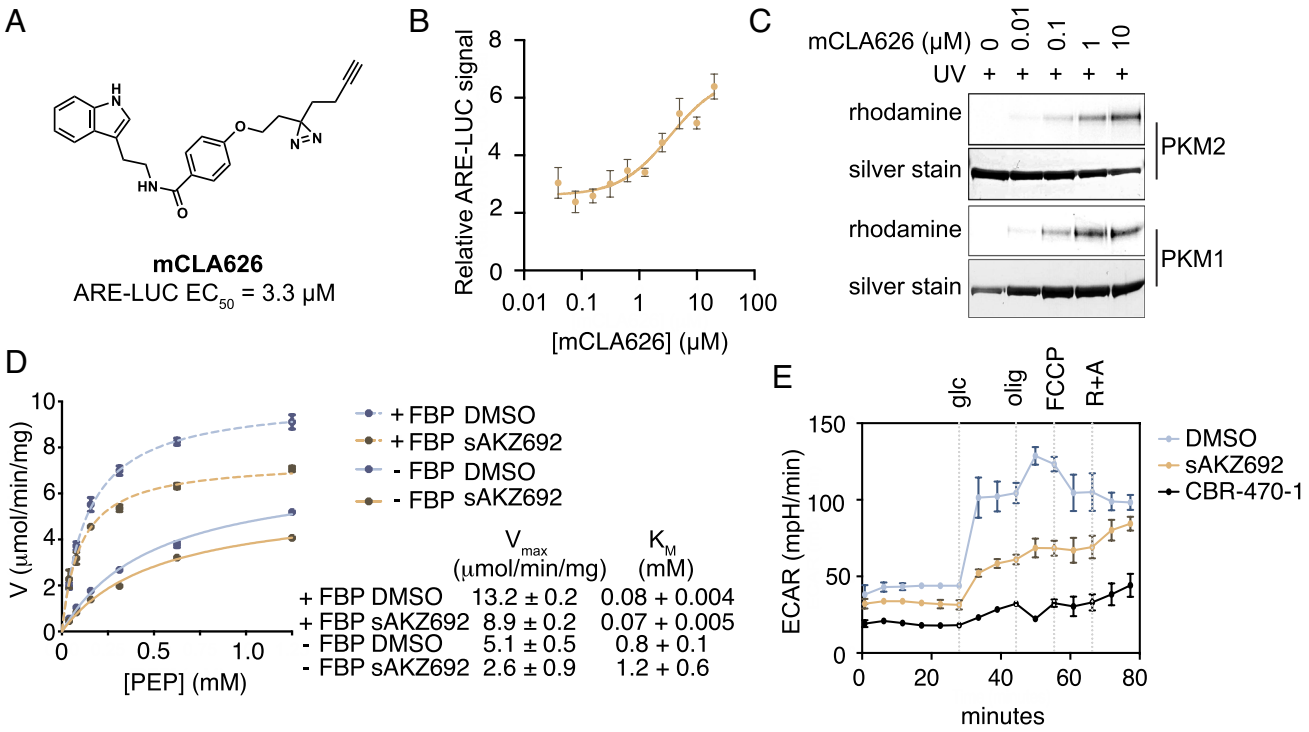

Fig. 2. sAKZ692 identified as a noncompetitive inhibitor of PKM2. (*A*) Structure of mCLA626, a photoactivatable affinity probe of sAKZ692. (*B*) Relative ARE-LUC signal in response to 24-h treatment of IMR32 cells treated with mCLA626 (n = 3; mean and SEM). (*C*) Representative gels of rhodamine azide-based labeling of recombinant PKM1 or PKM2 exposed to the indicated concentrations of mCLA626. (*D*) Plot of reaction rate and summary of V_{max} and K_M values of recombinant human PKM2 in the presence or absence of fructose bisphosphate (FBP; 100 μM) and sAKZ692 (20 μM) in response to increasing concentrations of phosphoenoylpyruvate (PEP). (*E*) Extracellular acidification rate from IMR32 cells treated with sAKZ692 or CBR-470-1 (20 μM each) as assessed by SeaHorse-based assay (glc = glucose, olig = oligomycin, FCCP = cyanide-p-trifluoromethoxyphenylhydrazone, R+A = rotenone and antimycin).

Consistent with a role in modulating PKM2 activity, sAKZ692 was found to markedly destabilize recombinant PKM2 protein in thermal denaturation assays, decreasing its melting temperature by more than 30 °C (dimethyl sulfoxide (DMSO) vehicle T_m = 62.8 °C; sAKZ692 T_m = 31.9 °C; *SI Appendix*, Fig. S2*C*). Likewise, sAKZ692 dose dependently destabilized PKM2 protein at 37 °C (*SI Appendix*, Fig. S2*D*), suggesting that the compound may compromise the activity of this enzyme in cells by modifying its tertiary or quaternary structure. sAKZ692 also inhibited the catalytic activity of PKM2 as assessed in a coupled assay measuring the oxidation of reduced nicotinamide adenine dinucleotide (NADH) by lactate dehydrogenase (Fig. 2*D*). sAKZ692 treatment did not alter the K_M (Michaelis constant) of PKM2 for phosphoenolpyruvate in the presence or absence of stimulating FBP; however, sAKZ692 did decrease the V_{max} in FBP-stimulated (8.9 vs. 13.2 μmol/min/mg) and -unstimulated (2.6 vs. 5.1 μmol/min/mg) states, indicating that the compound acts as a noncompetitive inhibitor of PKM2.

We next confirmed that sAKZ692 functionally inhibited PKM2 activity in IMR32 cells using a Seahorse assay (Agilent). Like the established PGK1 inhibitor CBR-470-1 (10 μM), sAKZ692 treatment (20 μM) blunted glycolytic output in basal and glucose-stimulated conditions in IMR32 cells, as measured by changes in extracellular acidification rate (ECAR, a surrogate measure of lactate generation; Fig. 2*E*) and oxygen consumption rate (OCR, a measure of oxidative respiration from glucose-derived pyruvate, *SI Appendix*, Fig. S2*E*). Lastly, we found that sAKZ692 treatment (20 μM) for 24 h in IMR32 cells decreased the levels of the active tetrameric form of PKM2, as assessed by western blotting for higher-molecular-weight adducts after cross-linking in situ with the chemical cross-linker DSS (disuccinimidyl suberate, *SI Appendix*, Fig. S2*F*). Together, these data demonstrate that sAKZ692 is a functional noncompetitive inhibitor of PKM2 activity in cells.

PKM2 Inhibition Activates NRF2 via the Buildup of a Reactive Metabolite. We next determined whether inhibiting PKM2 activity might result in NRF2 activation. From experiments involving transient cotransfection of HEK293T cells with shRNA and ARE-LUC reporter plasmids, four shRNAs targeting PKM2 promoted robust NRF2-driven reporter activation (Fig. 3*A*). Likewise, stable knockdown of PKM2 in IMR32 cells led to NRF2 transcriptional output, as measured by increased transcript levels of *NQO1* after 72 h of treatment (Fig. 3*B* and *SI Appendix*, Fig. S3 *A* and *B*). Importantly, both transient and stable shRNA-based knockdown of PKM2 resulted in a similar level of NRF2 activation to that of KEAP1 or PGK1 knockdown (Fig. 3 *A* and *B*), genetic manipulations shown to be NRF2 activating (10). Given the importance of PKM2 in central carbon metabolism, several pharmacological modulators of its activity have been developed. We found that Shikonin and Compound 3K (also called MDK4882 and PKM-IN-1, respectively), additional inhibitors of PKM2 reported in the literature (14, 15), dose dependently increased ARE-LUC reporter activity in IMR32 cells over a 24-h period (*SI Appendix*, Fig. S3 *C* and *D*). In contrast, stimulating PKM2 with the allosteric activators PF-06284674 or DASA had no effect on reporter output (*SI Appendix*, Fig. S3 *C* and *D*) (16, 17).

Given that we previously showed that inhibition of glycolysis results in NRF2 activation via buildup of a reactive metabolite (MGx), we hypothesized that a reactive glycolytic metabolite might also be responsible for sAKZ692-induced NRF2 activation. Indeed, treatment of IMR32 cells with exogenous GSH inhibited sAKZ692 (20 μM)-induced increases in *NQO1* transcript levels over a 24-h period (Fig. 3*C*). Likewise, treatment with 2-deoxyglucose, an inhibitor of the initial steps of glycolysis, as well as with GSH, concentration dependently inhibited increases in NQO1 protein levels in IMR32 cells treated with sAZK692 (20 μM; *SI Appendix*,

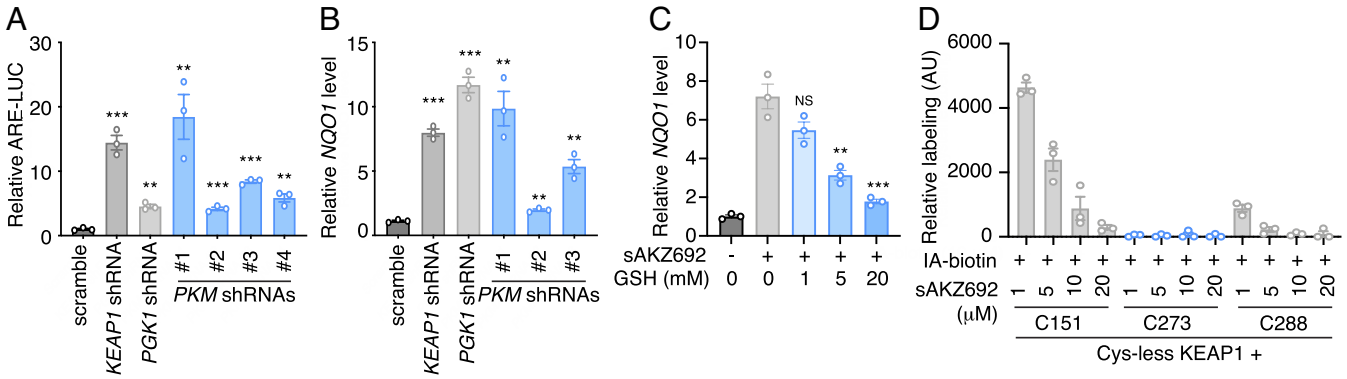

Fig. 3. Inhibiting PKM2 promotes preferential modification of C273 KEAP1 by a cysteine-reactive metabolite. (*A*) Relative ARE-LUC signal from HEK293T cells transiently transfected with pTI-ARE-LUC and plasmids encoding shRNAs silencing the indicated transcripts (scramble = nontargeting shRNA; mean and SEM). (*B*) Relative *NQO1* levels from IMR32 cells transduced with lentiviruses encoding shRNAs to the indicated transcripts after 72 h (scramble = nontargeting shRNA; mean and SEM). (*C*) Relative *NQO1* levels from IMR32 cells treated for 24 h with sAZK692 (20 μM) and the indicated concentrations of glutathione (GSH; $n = 3$; mean and SEM). (*D*) Densitometry-based quantification (arbitrary units) of competitive labeling by IA-biotin (10 μM) of anti-FLAG immunoprecipitated cysteine-less KEAP1 in HEK293T cells treated for 4 h with the indicated concentrations of sAKZ692 ($n = 3$; mean and SEM; NS = not significant; ***$P < 0.0005$, **$P < 0.005$, *t* test).

Fig. S3*E*). In contrast, treatment of IMR32 cells with nonthiol-reactive antioxidant ascorbic acid (5 mM) had no effect on NQO1 induction (*SI Appendix*, Fig. S3*E*), suggesting that sAKZ692 likely acts by promoting the buildup of a thiol-reactive metabolite derived from glycolysis.

Although an inhibitor of PKM2, an enzyme more downstream in glycolysis than PGK1, it is possible that sAKZ692 might also act by increasing the levels of the triose phosphate degradation product MGx, a metabolite that cross-links proximal KEAP1 molecules via MICA-based modification. From western blotting experiments involving transient overexpression of a FLAG-tagged KEAP1 transgene in HEK293T cells, we confirmed that treatment with the PGK1 inhibitor CBR-470-1 dose dependently increased the levels of dimeric KEAP1, a species indicative of MICA-based cross-linking (*SI Appendix*, Fig. S3*F*). Unlike CBR-470-1, sAKZ692 treatment did not result in dimer KEAP1 formation; instead, treatment decreased the background levels of dimeric KEAP1 (*SI Appendix*, Fig. S3*F*), suggesting that this compound likely acts by promoting accumulation of a KEAP1 thiol-reactive metabolite other than MGx.

Glyceraldehyde 3-Phosphate (Ga3P) Buildup Promotes the Nonenzymatic S-Lactoyl Modification of KEAP1. We next focused on identifying which cysteine residues of KEAP1 were modified in response to sAKZ692 treatment. We reasoned that use of a previously reported "cysteine-less" FLAG-tagged KEAP1 transgene (cys-less KEAP1) in which 11 commonly modified cysteines in KEAP1 were mutated (C151S, C226S, C257S, C273W, C288E, C319S, C434S, C489S, C613S, C622S, and C624S) might enable a residue-specific assessment of labeling (18). In this experimental paradigm, individual cysteine residues are reintroduced into the cys-less KEAP1 and then assessed for competitive labeling by treatment with iodoacetamide biotin (IA-biotin, 1 mM) after treatment with sAKZ692. The absence of anti-biotin-positive bands as assessed by western blotting from FLAG immunoprecipitated material indicates labeling of a given residue by a thiol-reactive metabolite induced by sAZK692 treatment. From an experiment involving cys-less KEAP1 with reintroduced C151, C273, or C288 [reported as the three predominant sensor residues in KEAP1 (19)], we found that treatment of HEK293T cells with a high concentration of sAKZ692 (20 μM) resulted in competitive labeling of all the three residues (*SI Appendix*, Fig. S3*G*). Performing the same experiment with several concentrations of sAKZ692 (1, 5, 10, and 20 μM) revealed that C273 was labeled across all concentrations of compound treatment, whereas C151 and C288 were labeled only at higher concentrations (Fig. 3*E* and *SI Appendix*, Fig. S3*H*). These results suggested that the relevant metabolite induced by sAKZ692 might broadly label sensor residues in KEAP1 but that C273 might be used as a potential handle for identifying the metabolite in question.

We next used liquid chromatography–tandem mass spectrometry to detect if any tryptic peptides in KEAP1 bear covalent modifications induced by sAKZ692 treatment. FLAG-tagged KEAP1 was expressed in HEK293T cells and then treated for 24 h with sAKZ692 (20 μM). We determined that C77, C288, C489, and C624/626 (tryptic fragment QIDQQNCTCGGR contains two cysteines that cannot be distinguished) uniquely bore a +72 Da modification only in the sAKZ692-treated samples, which we hypothesized corresponded to a metabolite-derived modification (*SI Appendix*, Fig. S4). Because this mass does not correspond to any known modification, we screened a repertoire of potentially cysteine-reactive metabolites related to glycolysis, including acetyl phosphate, MGx, 3 phosphoglycerate, Ga3P, dihydroxy acetone phosphate, 3-phosphohydroxypyruvate, and pyruvate, to determine whether they might label C273. Using cys-less KEAP1 C273 expressed in HEK293T cells, we found that among these metabolites (screened at 1 mM), only Ga3P competed for labeling by IA-biotin (Fig. 4 *A* and *B*). Importantly, we found that treatment of recombinant KEAP1 with Ga3P (1 mM) also resulted in the formation of a +72 Da adduct on KEAP1 tryptic peptides corresponding to C489 and C624/626 (*SI Appendix*, Fig. S5). Likewise, using a fluorescence-based kit for detecting Ga3P levels in cells (Abcam), we found that treatment of IMR32 cells with sAKZ692 resulted in a marked increase in Ga3P after 24 h of treatment (Fig. 4*C*). Lastly, we found that treatment of IMR32 cells with exogenous Ga3P (1 mM) in the presence of cationic lipid-based transfection reagent (FuGENE) resulted in NRF2 activation, as assessed by increases in ARE-LUC reporter activity at 24 h (Fig. 4*D*). Together, these data indicate that Ga3P is induced by sAKZ692 treatment and can activate NRF2 by modifying KEAP1, resulting in a +72 Da modification across several detectable cysteine residues.

To determine the mechanism by which Ga3P modifies cysteine thiols, we performed model reactions with a UV-detectable cysteine derivative (Fmoc-Cys-OMe). Forty-eight-hour room temperature incubation of Ga3P and Fmoc-Cys-OMe in phosphate buffer (pH 7.4) resulted in the formation of a +72 Da product, albeit in low yield, as detected by LC–MS (Fig. 4 *E*–*G*). Separation followed by ^{13}C NMR and two dimensional (2D) ^{1}H NMR analysis indicated the product corresponded to the lactate-modified species (Fig. 4 *H*–*J* and *SI Appendix*, Figs. S6–S9). Product assignment as the lactate

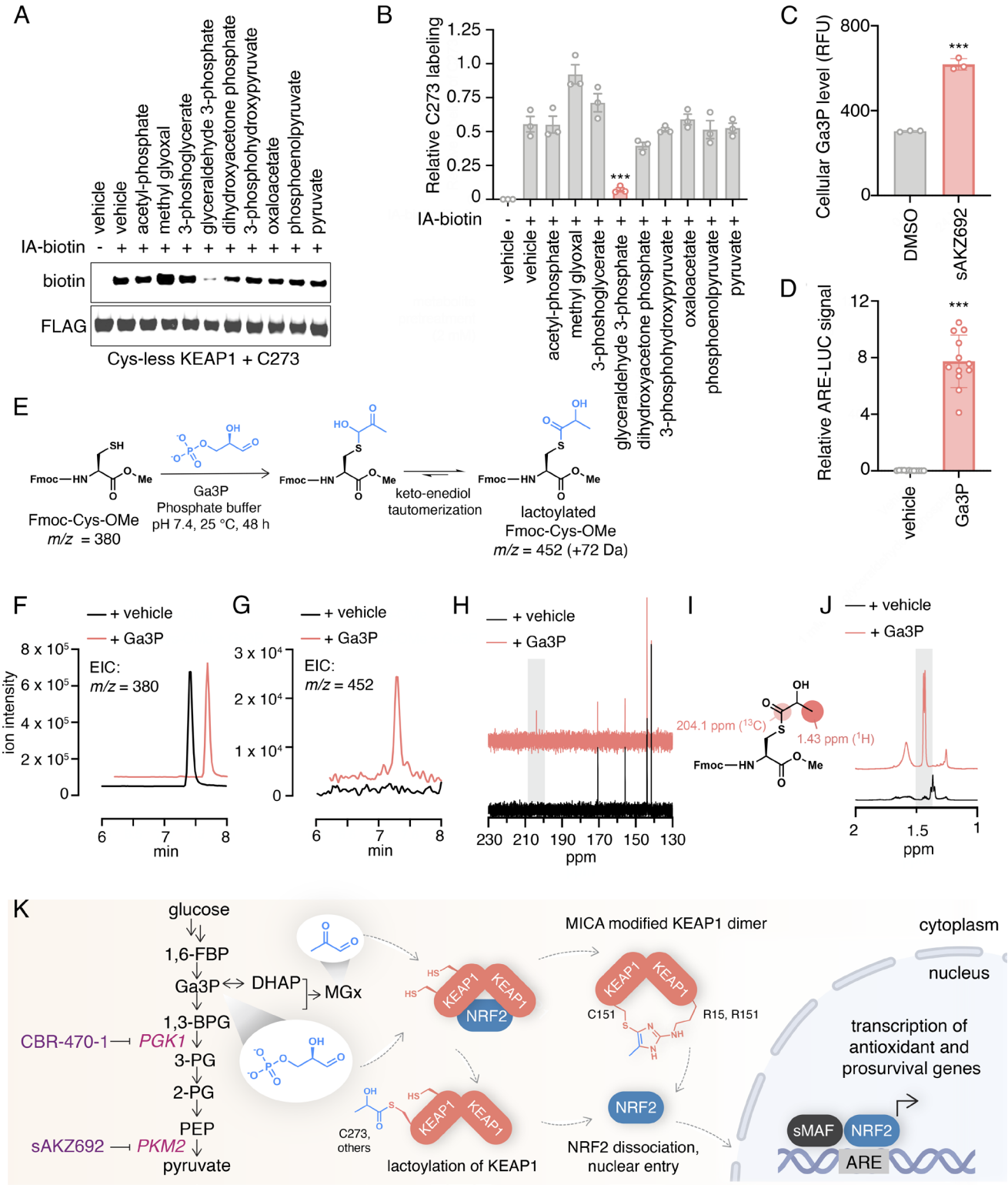

Fig. 4. Glyceraldehyde 3-phosphate nonenzymatically modifies KEAP1 to form an S-lactoyl species. Representative anti-biotin western blot (*A*) and densitometry-based quantification (*B*, arbitrary units) of labeling by IA-biotin (10 μM) of anti-FLAG immunoprecipitated Cys 273 containing cysteine-less KEAP1 treated with the indicated metabolites for 1 h in vitro (1 mM; $n = 3$; mean and SEM, $^{***}P < 0.0005$, *t* test). (*C*) Fluorescent kit-based quantification of Ga3P levels from IMR32 cells treated for 24 h with sAKZ692 (20 μM; $n = 3$; mean and SEM, $^{***}P < 0.0005$, *t* test). (*D*) Relative ARE-LUC signal from IMR32 cells treated with transfected Ga3P (1 mM) for 24 h ($n = 12$: mean and SEM, $^{***}P < 0.0005$, *t* test). (*E*) Schematic of reaction with Fmoc-Cys-OMe and Ga3P in phosphate buffer, indicating initial adduct formed followed by tautomerization to form the S-lactoyl modification. Extracted ion chromatograms (EICs) from aqueous vehicle or Ga3P-treated Fmoc-Cys-OMe corresponding to the starting material (*F*) or the formation of a +72 Da species (*G*). (*H*) ^{13}C NMR spectra of unmodified (*Bottom*) or Ga3P-modified (*Top*) Fmoc-Cys-OMe. Notable appearance of peak at 204.1 ppm corresponding to carbonyl carbon (*I*) is highlighted. (*J*) Isolated ^{1}H NMR spectra of the formation of unique doublet at 1.43 ppm (gray) corresponding to methyl protons in Ga3P-modified Fmoc-Cys-OMe (*Top*). (*K*) Schematic depicting the mechanism by which sAKZ692 activates NRF2 signaling in cells. In contrast to PGK1 inhibitor CBR-470-1 which leads to MGx buildup which results in a MICA-modified KEAP1 dimer, sAKZ692 promotes the buildup of Ga3P, resulting in overall S-lactoylation of numerous KEAP1 cysteine residues.

thiol ester was supported by the presence of 204.1 ppm peak in the ^{13}C NMR spectra corresponding to the carbonyl carbon of the formed thioester, as well as the presence of a new doublet in the ^{1}H NMR spectra corresponding to the terminal methyl group (Fig. 4 *H–J*). These results were corroborated by heteronuclear single-quantum coherence spectroscopy and double-quantum filtered correlated spectroscopy (*SI Appendix*, Figs. S10 and S11).

Lastly, to better mimic the context of the native protein, we performed in vitro reactions with Fmoc-Cys-OMe and an 8 amino acid model peptide corresponding to the natural sequence of KEAP1 near C273 (Ac-AVRCHSLT-NH_2). Ga3P treatment in fact resulted in a +72 Da adduct to the peptide in higher yield (*SI Appendix*, Fig. S12). Interestingly, we also observed the formation of a low abundance mass (962 Da) that corresponded to the intramolecular methyl imidazole-based modification of cysteine with the neighboring arginine (*SI Appendix*, Fig. S12). However, we did not observe the mass corresponding to this adduct in any cellular experiments, indicating that this species may be a potential thermodynamic product formed in vitro.

Discussion

To explore additional physiological mechanisms of NRF2 activation, we broadly interrogated a large chemical library for nonreactive inducers of ARE reporter activity. These efforts yielded sAKZ692, a tryptamine-based small molecule that selectively and robustly activates an NRF2 transcriptional program in cells. Unlike the majority of small-molecule NRF2 activators, which act covalently, sAKZ692 does not directly modify KEAP1 by alkylation. Instead, a target deconvolution campaign involving the use of a photoactivatable affinity probe and chemical proteomics identified the relevant target of sAKZ692 to be pyruvate kinase (PKM2).

PKM2 catalyzes the irreversible last step in glycolysis, a key metabolic regulatory node, and is capable of being allosterically regulated by metabolites. For example, fructose 1,6-bisphosphate, an upstream metabolite in glycolysis, promotes feedforward activation to augment PKM2 activity (12). Likewise, several amino acids, including phenylalanine, tryptophan, and alanine, have been shown to inhibit PKM2 by engaging a distinct site on the enzyme, signaling downstream catabolic sufficiency (20). Our study revealed sAZK692 to be a noncompetitive inhibitor of PKM2, decreasing its V_{max} in coupled enzyme assays. Given that multiple amino acids, like tryptophan, can allosterically inhibit PKM2 noncompetitively, it is conceivable that sAKZ692 may also occupy this allosteric binding site to inhibit enzymatic activity. This hypothesis is consistent with the observation that sAKZ692 still inhibits PKM2 activity when stimulated with FBP, which occupies a distinct allosteric site on the enzyme. Structural studies may shed insight into how sAKZ692 binds PKM2 and could provide a means to optimize this scaffold for increased potency. Unlike the commonly used PKM2 inhibitors, Shikonin and Compound 3K, sAKZ692 does not contain an internal napthylquinone that has the potential to deregulate redox metabolism. Together, these data suggest sAKZ692 will likely be a useful tool compound to interrogate the role of PKM2 in cells.

Mechanistic experiments revealed that sAKZ692 activates NRF2 by antagonizing the activity of PKM2, which leads to the buildup of a thiol-reactive glycolytic metabolite. Instead of promoting MGx accumulation and subsequent MICA-based KEAP1 modification as is the case with the PGK1 inhibitor CBR-470-1, sAZK692 treatment leads to the accumulation of Ga3P, a metabolite upstream of MGx. Increased Ga3P levels modify several cysteines in KEAP1 with a +72 Da increase in mass. sAKZ692 treatment leads to modification of C78, C288, C489, C624/626 as determined by mass spectrometry, a result which could be recapitulated when treating KEAP1 with Ga3P directly in vitro. We also observed that sAKZ692 competitively labels C151 and C273 residues in cell-based experiments, although we were unable to identify the +72 Da modification of these residues by mass spectrometry, likely due to the decreased detection of these tryptic fragments in our experiments. Nevertheless, these data indicate that inhibition of PKM2 activity in cells leads to modification of several cysteine sensor residues in KEAP1, resulting in increased NRF2 activity.

Model experiments strongly suggest that the +72 Da adduct induced by sAZ692 treatment corresponded to an overall S-lactoylation of cysteine with the end product being a thioester, a species we confirmed by 1D and 2D NMR. One potential explanation for the formation of the S-lactoyl modification might involve formation of 2-hydroxy acrolein as the reactive species, as Ga3P has been shown to readily eliminate phosphate to form this degradation product (21, 22). In this context, 1,2-nucleophilic attack of the thiolate to the acrolein aldehyde would result in a thioacetal that readily undergoes keto–enediol tautomerization to the more stable thioester S-lactoylated product. While energetically this mechanism is plausible, 2-hydroxy acrolein exists in solution in equilibrium with MGx. Likewise, the thioacetal formed upon 1, 2 addition is an intermediate that occurs in the reaction with MGx and would therefore likely favor MICA formation. Because the MICA adduct is not observed with Ga3P (*SI Appendix*, Fig. S3*F*), this mechanism is less likely. Another potential mechanism involves 1,2-addition of the Cys thiol group to the aldehyde group of Ga3P. The resulting thioacetal would preferentially eliminate the Cys thiol; however, loss of water (perhaps facilitated by the local protein backbone/environment) would likely lead to irreversible elimination of phosphate. The resulting hydration of the sulfenium moiety followed by enolization would then result in the formation of the thioester product. Future work will necessarily be required to define the mechanism of S-lactoyl modification by Ga3P.

This study demonstrates the ability of cysteine to be modified by "lactoylation". Lactoylation of lysine (N-lactoylation) has also been reported as a widespread modification in cells (23). Interestingly, N-lactoylation also proceeds nonenzymatically, although this modification occurs through acyl transfer from S-lactoyl-GSH, a metabolic product formed by the glyoxalase system (glyoxalases GLO1 and GLO2) which rids cells of excess MGx (24). It is possible that S-lactoylated cysteine residues may ultimately transfer their modifications to lysine, as has been shown with acetyl co-A-based cysteine acetylation (25), although we have not found evidence of this occurring in KEAP1. Likewise, given that GLO2 promotes the hydrolysis of lactoyl-GSH to form lactate, it is possible that GLO2 may serve an additional role removing thioester modifications of cysteine via hydrolysis (25). Like other reports with the KEAP1-reactive metabolites MGx and fumarate (26, 27), the development of alkyne probes of Ga3P coupled with chemical proteomics may help uncover the additional roles and the regulation of this unique modification.

This study further strengthens the interpathway communication between glycolysis and the KEAP1–NRF2 system by demonstrating that a second glycolytic metabolite, i.e., Ga3P, can directly modify KEAP1. Previously, we hypothesized that MGx-dependent NRF2 activation serves to keep the cellular levels of the electrophilic dicarbonyl metabolite MGx low, as NRF2 has been shown to transcriptionally up-regulate components of the glyoxalase system (10, 28). The demonstration that multiple metabolites of glycolysis can activate NRF2 activity by modifying KEAP1 supports the hypothesis that the cell has evolved this complex

communication network to protect itself from reactive metabolic intermediates. Beyond the glyoxalase system, NRF2 also reprograms cellular metabolism, up-regulating a number of pentose phosphate pathway (PPP) enzymes including glucose-6-phosphate dehydrogenase, transketolase, transaldolase, and phosphogluconate dehydrogenase (29). Upregulation of PPP enzymes by NRF2 may promote shunting of potentially toxic or unneeded glycolytic metabolites away from glycolysis and into the PPP. Given that PPP activity results in NADPH production, such a response would concomitantly decrease glycolytic flux while generating reducing equivalents in the form of NADPH for antioxidant processes. By having multiple glycolytic-reactive metabolites capable of signaling to the KEAP1, the cell may increase the number of contexts in which NRF2 may be activated as a homeostatic mechanism in cells. Finally, this work further underscores the utility of using unbiased forward pharmacological screens to uncover important cellular regulatory mechanisms.

Materials and Methods

Chemicals. Shikonin, Compound 3K, and DASA were obtained from Cayman Chemical. Metabolites were purchased from Sigma. PF-06284674 was purchased from Sigma. The synthesis of CBR-470-1 has been described. sAKZ692 and its analogs were purchased from ChemDiv. Photoactivatable affinity probe mCLA626 was synthesized in-house according to the procedures in *SI Appendix*. Fmoc-Cys-OMe was obtained from Combi-blocks. The octapeptide (Ac-AVRCHSLT-NH_2) was synthesized by GenScript.

Cell Lines and Culture. IMR32 and HEK293T cells were purchased from American Type Culture Collection and maintained in Dulbecc's Modified Eagle Medium (DMEM,Corning) supplemented 10% with fetal bovine serum (FBS, Gibco) and 1% penicillin-streptomycin (Pen Strep, Gibco). Cultures were regularly assessed for mycoplasma contamination using an in-house enzyme-linked immunosorbent assay (ELISA)-based detection service.

High-Throughput Screening. Four microliters of IMR32 cells (2,000 per well) in growth medium was dispensed per well in white 1536-well plates (Greiner) using a custom bottle valve and recirculatory system. To each well was then dispensed 2 μL of a transient transfection mixture containing 10 ng pTI-ARE-LUC, a previously reported ARE-LUC reporter plasmid, (10) and an equal ratio of DNA to the transfection reagent PEI. The next day, compounds were dispensed using an Echo acoustic liquid transfer device (Beckman Coulter). A full column containing 10 μM tert-butyl hydroquinone was used as a positive activation control. Another column containing only DMSO was used as a neutral stimulation control. The next day, 3 μL BrightGlo (diluted 1:3 in water) was added to each well. The plates were shaken, and luminance was recorded using a Viewlux instrument (PerkinElmer) with an exposure time of 60 s. Z′ values were typically between 0.1 and 0.5. IMR32 cells were used at passages 20 to 35 for screening.

ARE-LUC Reporter Assays. IMR32 cells were plated in 40 μL of growth medium (5,000 cells/well) in white 384-well plates (Greiner). The next day, each well was transfected with 100 ng pTI-ARE-LUC using FuGENE HD (4 μL per ug DNA) or 2 mg/mL polyethylenimine (PEI;1 μL per ug DNA) in freshly filtered 10 μL OptiMEM medium (Gibco). Twenty-four hours later, compounds were added (100 nL) via pintool transfer using a Bravo liquid handler (Agilent) outfitted with a VP Scientific pintool head. The next day, 30 μL BrightGlo (diluted 1:3 in water) was dispensed to each well, plates were shaken for 1 min, and the luminance signal was recorded using an Envision plate reader (PerkinElmer). For evaluating cytotoxicity in this format, 30 μL CellTiterGlo (diluted 1:6 in water) was added instead of BrightGlo and luminance signals were recorded similarly.

In Situ Labeling Experiments with Photoactivatable Affinity Probes. IMR32 cells ($2*10^6$ cells/well) were plated in 6-well plates in 2 mL of growth medium. After 24 h, the wells were washed with phenol red-free DMEM (Gibco) twice. To each well was dispensed, 2 mL phenol red-free DMEM and mCLA626 at the indicated concentrations as DMSO solutions for 30 min at 37 °C. After irradiation with long-wave UV (365 nm) at 4 °C for 15 min, cells were washed with PBS (phosphate-buffered saline, Corning) twice, scraped into 0.2 mL PBS, and lysed by sonication. Insoluble material was removed by centrifugation (13,000 g for 5 min at room temperature). Prepared lysate in PBS (50 μL at 1 mg/mL) was incubated with Click reagent mix (1 μL of 1.25 mM rhodamine azide in DMSO, 1 μL of 50 mM $CuSO_4$ in H_2O, 1 μL of 50 mM TCEP in water, 3 μL of 1.7 mM TBTA in tBuOH:DMSO 4:1) at room temperature for 1 h in the dark. The reaction mixture was precipitated in cold methanol and the pellet was redissolved in PBS containing 0.1% SDS. The resulting sample was mixed with loading buffer and separated via sodium dodecyl sulfate–polyacrylamide gel electrophoresis (SDS-PAGE).

Streptavidin Enrichment for Target Identification. Confluent IMR32 cells in a 10-cm tissue culture dish were washed with phenol red-free DMEM (Gibco) twice. The cells were treated with 5 μM mCLA626 or with DMSO in phenol red-free DMEM and incubated at 37 °C for 30 min. After irradiation with long-wave UV (365 nm) at 4 °C for 15 min, the cells were washed with PBS twice, scraped into 0.8 mL PBS, and then lysed by sonication. Insoluble materials were removed by centrifugation. Two 1.5 mL tubes per biological sample containing 0.5 mL of 2 mg/mL lysate were incubated with Click reagent mix (30 μL of 1.7 mM TBTA in tBuOH:DMSO 4:1, 10 μL of 50 mM $CuSO_4$ in H_2O, 10 μL of 50 mM TCEP in H_2O, 2.5 μL of 20 mM biotin-PEG3-N_3) at room temperature for 1 h. The reaction mixture was precipitated in cold methanol and the pellet was redissolved in 1 mL PBS containing 0.6% sodium dodecyl sulfate (SDS). The resulting samples were combined to make a 2 mL mixture, which was then incubated with 220 μL streptavidin beads in 10 mL PBS for 24 h on a rotator at room temperature. The beads were pelleted by centrifugation at 2,000 g for 1 min and then washed with 10 mL of 0.1% SDS in PBS twice, 10 mL of PBS twice, and then 10 mL of water twice. Two hundred microliters of 2× sample buffer with 10% beta-mercaptoethanol was added to the beads, and the beads were boiled at 99 °C for 15 min. Supernatant was analyzed by anti-biotin western blot and silver stain. Excised bands were sent to the Scripps Research proteomics core for MS/MS-based identification of present proteins.

Recombinant Protein Labeling. PKM2 (SAE0021, Sigma) was reconstituted in PBS containing 30% glycerol to a final concentration of 2 mg/mL. One microgram PKM2 in 50 μL PBS was incubated with the indicated concentrations of mCLA626 at 37 °C for 1 h, and then irradiated with long-wave UV (365 nm) for 10 min at 4 °C. The sample was then reacted and incubated with rhodamine azide click reagent master mix at room temperature for 1 h and then the samples were resolved by SDS-PAGE. Gels were incubated in 10% ethanol for 1 h before imaging fluorescence on a ChemiDoc instrument (Bio-Rad). The gel was then stained with a Silver Stain Kit from Pierce to assess equal loading of lanes.

Seahorse Assays. Ninety-six-well Seahorse plates were coated with 50 μg/mL poly-d-lysine (Sigma) in PBS at 37 °C for 30 min and washed twice with water. 50 μg/mL laminin in PBS was then added and the plate was incubated at 37 °C for an additional 30 min before drying the wells completely. A total of 20,000 IMR32 cells were then plated per well in 100 μL of growth medium. After 24 h, 20 μM CBR-470-1 or AKZ692 was delivered to each well. The next day, cells were washed twice in assay buffer (Seahorse DMEM, 2 mM glutamine, no glucose and no pyruvate, pH 7.4) and incubated for 1 h in a CO_2-free incubator. The cells were sequentially treated with 10 mM glucose and 1 mM pyruvate, 1 μM oligomycin, 1 μM FCCP, and 2 μM rotenone with 2 μM antimycin A and the OCR or ECAR was measured using an Agilent Seahorse XF instrument.

Recombinant Enzyme Activity Assays. 2× assay buffer containing 4 mM ADP, 40 U/mL lactate dehydrogenase, 20 mM $MgCl_2$, 200 mM KCl, 1 mM DTT, and 1 mM NADH was prepared in PBS (without Ca, Mg). Phosphoenolpyruvate was prepared in 2× assay buffer at the indicated concentrations, and 50 μL of this solution was then added to each well in black clear bottom 96-well plates (Corning). 0.002 mg/mL PKM2 in PBS containing 1 mM DTT was incubated at 37 °C for 30 min in the presence or absence of 1 mM fructose-1,6-bisphosphate and 20 μM AKZ692. 50 μL of PKM2 solution was added to each well. After agitating the plate for 10 s, absorbance at 340 nm was read for 2 min using a SpectraMax 250 plate reader (Molecular Devices).

Data, Materials, and Software Availability. RNA sequencing data have been deposited in NCBI GEO (https://www.ncbi.nlm.nih.gov/geo/query/acc.cgi?acc=GSE230577) (30).

ACKNOWLEDGMENTS. We thank Kristen Williams for assistance with manuscript preparation and submission, Linh Truc Hoang of the Scripps Research Center for Metabolomics for assistance with mass spectrometry-related experiments, and Brittany Sanchez and Jason Chen of the Scripps Automated Synthesis Facility for assistance with chemical purification. This work was supported by the NIH (GM146865 to M.J.B.).

1. L. Ibrahim *et al.*, Defining the functional targets of cap'n'collar transcription factors NRF1, NRF2, and NRF3. *Antioxidants (Basel)* **9**, 1025 (2020).
2. G. P. Sykiotis, D. Bohmann, Stress-activated cap'n'collar transcription factors in aging and human disease. *Sci. Signal* **3**, re3 (2010).
3. Q. Ma, Role of nrf2 in oxidative stress and toxicity. *Annu. Rev. Pharmacol. Toxicol.* **53**, 401–426 (2013).
4. L. Baird, M. Yamamoto, The molecular mechanisms regulating the KEAP1-NRF2 pathway. *Mol. Cell Biol.* **40**, e00099-20 (2020).
5. A. T. Dinkova-Kostova, R. V. Kostov, P. Canning, Keap1, the cysteine-based mammalian intracellular sensor for electrophiles and oxidants. *Arch Biochem. Biophys.* **617**, 84–93 (2017).
6. D. Malhotra *et al.*, Global mapping of binding sites for Nrf2 identifies novel targets in cell survival response through ChIP-Seq profiling and network analysis. *Nucleic Acids Res.* **38**, 5718–5734 (2010).
7. J. Adam *et al.*, Renal cyst formation in Fh1-deficient mice is independent of the Hif/Phd pathway: Roles for fumarate in KEAP1 succination and Nrf2 signaling. *Cancer Cell* **20**, 524–537 (2011).
8. A. Ooi *et al.*, An antioxidant response phenotype shared between hereditary and sporadic type 2 papillary renal cell carcinoma. *Cancer Cell* **20**, 511–523 (2011).
9. E. L. Mills *et al.*, Itaconate is an anti-inflammatory metabolite that activates Nrf2 via alkylation of KEAP1. *Nature* **556**, 113–117 (2018).
10. M. J. Bollong *et al.*, A metabolite-derived protein modification integrates glycolysis with KEAP1-NRF2 signalling. *Nature* **562**, 600–604 (2018).
11. J. Jo *et al.*, Discovery and SAR studies of 3-amino-4-(phenylsulfonyl)tetrahydrothiophene 1,1-dioxides as non-electrophilic antioxidant response element (ARE) activators. *Bioorg. Chem.* **108**, 104614 (2021).
12. Z. Zhang *et al.*, PKM2, function and expression and regulation. *Cell Biosci.* **9**, 52 (2019).
13. T. L. Dayton, T. Jacks, M. G. Vander Heiden, PKM2, cancer metabolism, and the road ahead. *EMBO Rep.* **17**, 1721–1730 (2016).
14. J. Chen *et al.*, Shikonin and its analogs inhibit cancer cell glycolysis by targeting tumor pyruvate kinase-M2. *Oncogene* **30**, 4297–4306 (2011).
15. X. Ning *et al.*, Discovery of novel naphthoquinone derivatives as inhibitors of the tumor cell specific M2 isoform of pyruvate kinase. *Eur. J. Med. Chem.* **138**, 343–352 (2017).
16. D. Anastasiou *et al.*, Inhibition of pyruvate kinase M2 by reactive oxygen species contributes to cellular antioxidant responses. *Science* **334**, 1278–1283 (2011).
17. S. Arora *et al.*, A perspective on medicinal chemistry approaches for targeting pyruvate kinase M2. *J. Med. Chem.* **65**, 1171–1205 (2022).
18. T. Suzuki *et al.*, Molecular mechanism of cellular oxidative stress sensing by Keap1. *Cell Rep.* **28**, 746–758.e4 (2019).
19. R. Saito *et al.*, Characterizations of three major cysteine sensors of Keap1 in stress response. *Mol. Cell Biol.* **36**, 271–284 (2016).
20. M. Yuan *et al.*, An allostatic mechanism for M2 pyruvate kinase as an amino-acid sensor. *Biochem. J.* **475**, 1821–1837 (2018).
21. M. Schumperli, R. Pellaux, S. Panke, Chemical and enzymatic routes to dihydroxyacetone phosphate. *Appl. Microbiol. Biotechnol.* **75**, 33–45 (2007).
22. P. J. Thornalley, The glyoxalase system: New developments towards functional characterization of a metabolic pathway fundamental to biological life. *Biochem. J.* **269**, 1–11 (1990).
23. D. O. Gaffney *et al.*, Non-enzymatic lysine lactoylation of glycolytic enzymes. *Cell Chem. Biol.* **27**, 206–213.e6 (2020).
24. D. O. Farrera, J. J. Galligan, The human glyoxalase gene family in health and disease. *Chem. Res. Toxicol.* **35**, 1766–1776 (2022).
25. A. M. James *et al.*, Non-enzymatic N-acetylation of lysine residues by acetylCoA often occurs via a proximal S-acetylated thiol intermediate sensitive to glyoxalase II. *Cell Rep.* **18**, 2105–2112 (2017).
26. J. S. Coukos, C. W. Lee, K. S. Pillai, K. J. Liu, R. E. Moellering, Widespread, reversible cysteine modification by methylglyoxal regulates metabolic enzyme function. *ACS Chem. Biol.* **18**, 91–101 (2022).
27. R. A. Kulkarni *et al.*, A chemoproteomic portrait of the oncometabolite fumarate. *Nat. Chem. Biol.* **15**, 391–400 (2019).
28. M. Xue *et al.*, Transcriptional control of glyoxalase 1 by Nrf2 provides a stress-responsive defence against dicarbonyl glycation. *Biochem. J.* **443**, 213–222 (2012).
29. Y. Mitsuishi *et al.*, Nrf2 redirects glucose and glutamine into anabolic pathways in metabolic reprogramming. *Cancer Cell* **22**, 66–79 (2012).
30. Y. Ko, L. Ibrahim, M. Bollong, S-lactoyl modification of KEAP1 by a reactive glycolytic metabolite activates NRF2 signaling. NCBI Gene Expression Omnibus. https://www.ncbi.nlm.nih.gov/geo/query/acc.cgi?acc=GSE230577. Deposited 24 April 2023.